HNPS Advances in Nuclear Physics

Vol 6 (1995)

HNPS1995

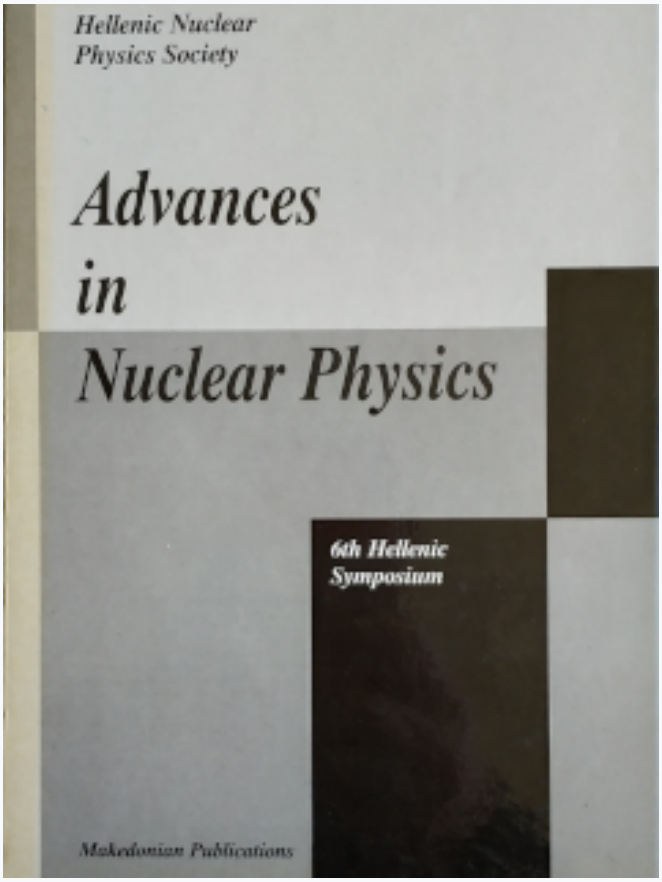

Shell model calculations in the A ~ 100 mass region

P. Divari, L. D. Skouras

doi: 10.12681/hnps.2931

Shell model calculations in the $A \sim 100$ mass region.

P Divari and L D Skouras

Institute of Nuclear Physics, N.C.S.R. Demokritos GR-15310 Aghia Paraskevi, Greece

Abstract

The properties of nuclei with $39 \leq Z \leq 47$ and $N = 51 - 52$ are investigated in large scale shell-model calculations. The doubly closed nucleus $^{100}_{50}$Sn is selected as the reference state and the nuclei under examination are described in terms of proton holes and one up two neutrons outside the inert core. The proton holes are distributed in a model space consisting of the orbitals $g_{9/2}$, $p_{1/2}$, $p_{3/2}$ while $f_{5/2}$ is sometimes also considerd. Similary the model space for the neutron particles includes the orbitals $g_{7/2}$, $d_{5/2}$, $d_{3/2}$, $s_{1/2}$ and in certain cases $h_{11/2}$. The effective two-body interaction and the matrix elements of the effective operators were determined by introducing second-order corrections to the Sussex matrix elements. The single proton holes as well as the single-neutron energies were treated as parameters which were determined by least-squares fit to the observed levels of $39 \leq Z \leq 47$, $N = 50$ and $N = 51$ respectively. The results of the calculation were found to be in satisfactory agreement with experimental data and this enable us to make predictions about the properties of some exotic nuclei in the vicinity of ^{100}Sn.

1 Introduction

With the development of new experimental techniques it has become possible to study the very proton-rich nuclei. Studies of the $^{98}_{51}$Ag, $^{99}_{51}$Cd and $^{100}_{50}$Sn should be available in the near future. The experimental study of nuclei in the vicinity of $^{100}_{50}$Sn provides a nice area for comparisons with nuclear structure models. Because the 50 protons and 50 neutrons correspond to a well-established shell closure, it is convenient to use the doubly closed nucleus $^{100}_{50}$Sn as the closed inert core and study configurations with few particles and holes outside of it. So the effects of variation of the model space can be studied systematically.

Talmi and Unna [1] made the first treatment of the $N = 50$ nuclei in 1960. They determined effective interaction within a model space $g_{9/2}$ and $p_{1/2}$ by

least-squares fit to the then known experimental energy levels. Several other shell model studies of nuclei Z, N$\leq$ 50 followed the work of Talmi and Unna. Gazzaly [2-3] *et al* studied ^{90}Zr in the extented model space $g_{9/2}$, $p_{1/2}$, $p_{3/2}$ and $f_{5/2}$ assuming $^{78}_{28}$Ni as core and using an empirical interaction. The approach of Gazzaly *et al* has been adopted by Ji and Wildenthal in their sudies [4-6] on the properties of the $N = 50$ nuclei. Recently successful theoretical investigations [7-10] on the mass region $A = 80 - 100$, were realized in a model space consisting of the $g_{9/2}$, $p_{1/2}$, $p_{3/2}$ and $f_{5/2}$ proton and neutron hole orbitals outside the doubly-closed core $^{100}_{50}$Sn. The wavefunctions of those calculations were used to determine the double β decay of Ge, Se, Sr and Kr isotopes. Skouras and Dedes [11] made also an attempt to explain the observed even-parity spectrum and transitions rates of ^{95}Tc. In this shell-model approach three valence protons were restricted to the $g_{9/2}$ orbital, while full configuration mixing has been assumed for the two valence neutrons which are allowed to take all possible values in the $d_{5/2}$, $d_{3/2}$, $s_{1/2}$ and $g_{7/2}$ orbitals. Despite the success these calculations have had their model space for the valence proton particles was very restricted for the description of nuclei with Z$\geq$ 38, specially for the nuclei in the middle of the proton shell.

In this work an attempt is made to explain the energy spectra and the decay properties of nuclei $39 \leq Z \leq 47$, $N = 51 - 52$. Our calculation differs from the previously mentioned shell-model calculation of Skouras and Dedes in respect of full configuration mixing between protons is allowed. For this reason the nucleus ^{100}Sn is selected as the inert core outside of which proton-holes and a sigle-neutron are distributed in two separate model spaces. The determination of effective two-hole as well as particle-hole interactions are evaluated in a realistic way. Details of the model spaces we consider are discussed in sec. 1 while the results of the calculation are presented in sec. 2.

2 Details of the calculation

As outlined in sect.1, in the present work we assume a ^{100}Sn inert core considering proton holes distributed in the $g_{9/2}$, $p_{1/2}$, $p_{3/2}$ orbitals and a single neutron in the $g_{7/2}$, $d_{5/2}$, $d_{3/2}$ and $s_{1/2}$ of the harmonic oscillator potential. The large number of orbitals involved in the above model spaces produce exceedingly large dimansions for the energy matrices. For this reason the weak-coupling approximation has been adopted. Thus the shell-model Hamiltonian which describes the nuclei $39 \leq Z \leq 47$, $N = 51 - 52$ can be expressed as a sum of three terms

$$H = H_h + H_p + V_{hp} \tag{1}$$

where H_h and H_p denote the Hamiltonians in the proton and neutron spaces respectively, while V_{hp} represents the interaction between proton-holes and the neutron-particle. Each of the H_h and H_p terms consists of a single-particle and a two-body term.

The basis vectors of the weak-coupling calculation have the form

$$||n_h\mu_h j_h^{-1}\rangle \ , |n_p\mu_p j_p\rangle \ ; J\rangle \tag{2}$$

where $|n_h\mu_h j_h^{-1}\rangle$ denotes the proton hole wave functions, while $|n_p\mu_p j_p\rangle$ the corresponding neutron particle wave functions. The indcies n_h and n_p denote the number of protons and neutrons, while μ_h as well as μ_p distinguishe the orthogonal states which all correspond to the same j_h and j_p values respectively. So the first step towards the calculation of H is the determination of term H_h. For this reason we distributed, as mentioned before, proton holes in the model space consisting of the orbitals $g_{9/2}$, $p_{1/2}$ and $p_{3/2}$. After systematic analysis for the best choice of proton holes model space it was found that the above model space was not so realistic for the description of nuclei in the middle of the proton shell. On the other hand the inclusion of $f_{5/2}$ orbit within the proton holes model space gave rise to strong configuration mixing with the other orbits of the space. So we have considered two model spaces. The model space $g_{9/2}$, $p_{1/2}$, $p_{3/2}$, hearafter to be referred to as $model-1$, quite realistic for the description of the nuclei $42 \leq Z \leq 47$ and another one consisting of the orbitals $g_{9/2}$, $p_{1/2}$, $p_{3/2}$ and $f_{5/2}$ referred as $model-2$, proper for the investigation of the nuclei $39 \leq Z \leq 41$ (see Fig.1).

For the determination of H_h it is demanded the calculation of the two-hole effective interaction [7-8]. This is realized by perturbation theory introducing second order corrections, in a space of $2\hbar\omega$ excitations above the model space. The NN interaction we considered was the Sussex [12] pontential, while the diagrams we have computed are shown in Fig.2. We have also assumed harmonic oscillator pontential as the zero-order single-particle spectrum, for which the oscillator parameter $b = (\hbar/m\omega)^{1/2}$ has been given the value 2.1 fm appropriate for this mass region. In Table 1 we list a selection of matrix elements of the two - hole effective interaction for the model spaces $model-1$ and $model-2$. As we can see the effects of $f_{5/2}$ orbit on the renormalization of the $model-1$ interaction are, in second order, very small.

The single hole-energies can not be taken from experiment, since the nuclei $^{99}_{49}$In and $^{101}_{50}$Sn are far from the stability line, so they were treated as parametres which were determined by a least-squares fit to the observed energy levels. Specifically we made two fitting procedures. The first one includes nuclei from the mass region $42 \leq Z \leq 47$, $N = 50$ and the second one the nuclei $39 \leq Z \leq 41$, $N = 50$. Under these circumstances two sets of single-hole energies

are obtained for the two model spaces we have considered. The first set is

$$\epsilon_{9/2} = 0.00, \quad \epsilon_{1/2} = 1.21, \quad \epsilon_{3/2} = 2.18 \tag{3}$$

and the second one is

$$\epsilon_{9/2} = 0.00, \quad \epsilon_{1/2} = 1.80, \quad \epsilon_{3/2} = 3.30, \quad \epsilon_{5/2} = 6.28 \quad (in \quad MeV) \tag{4}$$

It is interestig to note comparing the above two sets of energies, that the additional $f_{5/2}$ orbital increaces the energy of the $p_{1/2}$ state by about 600 keV while the $p_{3/2}$ state by about 1 MeV. All the above single-particle energies have been computed with respect to $g_{9/2}$ orbital.

The single-neutron particle is placed in the model space consisting of the orbitals $g_{7/2}$, $d_{5/2}$, $d_{3/2}$ and $s_{1/2}$ but we have also examined the effects introduced by the inclusion of the $h_{11/2}$ within this model space. The restricted neutron model space will be referred as $model-3$ while the extened one as $model-4$ (see Fig.1). For the determination of the single-neutron energies we followed the same procedure as for the proton holes. Namely we made a least-squares fit including available experimental data from the mass region $39 \leq Z \leq 47$, $N = 51$ into the fitting procedure. Thus treating two model spaces for the single-neutron, we can obtain two sets of single-particle energies:

$$\epsilon_{5/2} = 0.000, \quad \epsilon_{7/2} = 0.081, \quad \epsilon_{3/2} = 2.190, \quad \epsilon_{1/2} = 1.905 \tag{5}$$

and

$$\epsilon_{5/2} = 0.000, \quad \epsilon_{7/2} = -0.003 \quad \epsilon_{3/2} = 2.420, \quad \epsilon_{1/2} = 1.910$$
$$\epsilon_{11/2} = 3.360 \quad (in \quad MeV) \tag{6}$$

The additonal $h_{11/2}$ orbital has little effect on the energies of the $s_{1/2}$ and $g_{7/2}$ but increaces the energy of $d_{3/2}$ orbital by about 200 keV.

The effective two-particle interaction has been calculated to second order permitting excitations in a space of $2\hbar\omega$ above the neutron model space. Finally, the V_{hp} part of the shell-model Hamiltonian (1) has been determined, in the usual manner, by considering second-order corrections, in the space of $2\hbar\omega$ excitations, to the proton-hole, neutron-particle interaction.

In a similar manner to the perturbative determination of effective interaction, we have also determined effective proton - hole as well as neutron - particle reduced matrix elements which were calculated by perturbation theory introducing second order corrections. As an example of this calculation we list in Table 2 the reduced matrix elements corresponding to single-neutron patricle states, while in Fig.3 we show the correspondig diagrams. In the first column we always obtain the values correspond to the bare operators. As we can see comparing the first column with the other two, the matrix elements are both

sizable and state-dependent. On the contrary the reduced matrix elements in the two neutron model spaces *model*-3 and *model*-4 are quite similar. It is also intresting to be emphasized the necessity of including $h_{11/2}$ orbit within the neutron model space in order to describe transitions like M2, M4, E3 and E5 because of the spin and parity conservation.

3 Results of the calculation

In this section we present a selection of the results of our shell-model calculation on the $39 \leq Z \leq 47$, $N = 51 - 52$ nuclei and compare them with the experimental data.

In Fig.4 we show the experimental [13,14] and theoretical spectra of ^{97}Pd and ^{95}Ru. For these nuclei a detailed comparsion with experiment is difficult to be done due to the many uncertainties that still exist in the experimental spectra even among the low-lying levels. Most experimental states up to 2.5 MeV of excitation are reproduced in the theoretical spectra within 100-200 keV and in addition our calculation predicts the presence of several others. It is also interesting to note that our calculation confirms the existence of some tentative high spin states in the experimental spectrum of ^{95}Ru above 2.5 MeV like the possible $15/2^-$, $17/2^-$, $19/2^-$ and $25/2^+$. At the same time in the experimental spectra of ^{97}Pd and ^{95}Ru there are appear states for which no spin and parity assignments have been made. Until such assignments have been established the comparison between theory and experiment can not be complete.

Fig.5 shows for comparison the theoretical and experimental spectra [15,16] of the nuclei ^{92}Nb and ^{94}Tc up to 2 MeV. For higher excitations the experimental knowledge of these two nuclei is still very incomplete and thus a detailed comparison between theory and experiment is not possible. As may be seen in Fig.3, all low lying states below 1 MeV are predicted by our calculation within 100-200 keV. Specifically in the experimental spectrum of ^{92}Nb there are appear two 1^+ states, one at 1.08 MeV and another one at 0.97 MeV. However the calculation predicts only one such state at 0.63 MeV. Until further experimental information is possible a detailed comparison is not feasible.

Fig.6 shows the experimental [17,18] and theoretical spectra of ^{91}Zr and ^{93}Mo. As Fig.6 shows, our calculation reproduces all the observed states of ^{91}Zr, within 100-400 keV. However there are some interesting features to be observed like:
i)The description of the spectrum with the restricted model space of neutrons accounts for all excited $11/2^-$ states within 500 keV up 1 MeV higher of the observed states. On the contrary the inclusion of $h_{11/2}$ orbital within the

neutron model space reproduces them to within 100 up 400 keV of the observed levels. This can be attributed to the fact that these states are mainly described, according to the weak the coupling approximation we have adopted, by the coupling of the ground state of ^{90}Zr with a single neutron at $h_{11/2}$. Namely the perdominant componet in the $11/2^-$ wave functions of ^{91}Zr comes from the basis vector

$$||n_h = 10, \mu_h = 1, j_h^{-1} = 0^+\rangle \ , j_p = 11/2^-; J = 11/2^-\rangle \qquad (7)$$

ii) our calculation accounts for an additional $11/2^+$ at 2.61 MeV. It would be a very useful test for our calculation a more extented experimental investigation for the excistence or not of such a state.
iii) A possible $1/2^-$ state in the observed spectrum at 2.35 MeV is predictied by our calculation 1 MeV higher. If the existence of such a state is confirmed then the good agreement between theory and experimet could be partially destroyed.
iv) All high spin states above 2.5 MeV like the $21/2^+$, $13/2^-$ and $17/2^+$ are accounted for to within 300 keV.

In Fig.6 we also show the experimental and theoretical spectrum of ^{93}Mo up to 2.5 MeV. Our calculation accounts satisfactorily for all the observed states up to 2.5 MeV. The agreement between theory and experiment is extremely good for both negative and positive parity states, since all the observed states are reproduced within 100-200 keV.

The spectra of the nuclei ^{96}Rh, and ^{98}Ag are shown in Fig.7. Most experimental states [19,20] up to 2.5 MeV of excitation are reproduced in the theoretical spectra within 100-400 keV. It is worth noting that our calculation accounts for all the observed high spin states of ^{96}Rh that appear above 2 MeV (see Fig.8). Then for most levels like the possible 11^+, 11^-, 12^-, 14^+, 13^-, 14^-, 15^+ and 15^- the difference between observed and calculated excitation energy does not exeed 200 MeV. Besides our calculation predicts the presence of more additional states in both ^{98}Ag and ^{96}Rh spectrum. More systematic experimental investigation for the existence or not of those levels would provide a very useful test of the present calculation.

Fig.9 shows the theoretical and experimental [20,19] spectra of the nuclei ^{98}Pd and ^{96}Ru. Since the experimental knowledge of them are very incomplete a detailed comparison between theory and experiment is very difficult to be done. For all that, some useful conclusions can be drawn. In spectrum of ^{98}Pd our model seems to reproduce all low lying states 2^+, 4^+, 6^+ and 5^- within 100-200 keV. For the upper lying states our model reproduce the first excited 10^+ at 3.21 MeV and a second one at 3.70 MeV. In the experimental spectrum there is only one possible 10^+ state at 3.64 MeV. The same situation is being observed at the excited levels 14^+ and 12^+. Specifically our model predicts a first excited 12^+ at 4.06 MeV and a second one at 4.38 MeV, as well as two

excited 14^+ at 5.30 and 5.60 MeV. In the experimental spectrum there appear only two states, a possible 12^+ at 4.44 MeV and a possible 14^+ at 5.69 MeV.

Similar conclusions can be drawn for the spectrum of nucleus ^{96}Ru. Our model accounts satisfactorily for the experimental states up to 2.20 MeV, while above 2.20 MeV there is a great uncertainty to the observed spectrum. In general there is a good agreement to the predictions of the high spin states 9^-, 12^+, 10^-, 14^+ and 16^+ which are reproduced within 100 - 200 keV.

In Fig.10 we present experimental and theoretical spectra of the nuclei ^{95}Tc and ^{93}Nb [14,18]. As Fig.10 shows the agreement between experiment and theory of the above two nuclei is very satisfactory. Especially good agreement is being observed for the high spin states of ^{95}Tc like those of $17/2^+$, $15/2^+$, $13/2^-$, $19/2^+$ $17/2^-$, $21/2^+$, $21/2^-$, $25/2^-$, $25/2^+$ and $29/2^+$ which are reproduced within 100 keV. Also as Fig.10 shows our calculation reproduce in a very satisfactory manner the excitation energies of most of the observed levels of ^{93}Nb, although the experimental data are very doubtful. It is also interesting at the future experimental resecrches, that our model pedicts above 2 MeV the existence of a sequence of states with negative parity like $13/2^-$, $11/2^-$, $17/2^-$, $15/2^-$ $21/2^-$, $19/2^-$ and $25/2^-$.

Fig.11 shows the spectra of the even-even nuclei ^{92}Zr and ^{94}Mo [15,16]. The great majority of states on the first of these two nuclei, are accounted for quite satisfactorily by our model with only two exceptions. The first one concerns the observed 3^- state. The main reason for which our model fails to account for the observed 3^- state is the following:

As we have already mentioned before a given wave function is expanded in a weak coupling basis of the form (2). In the case of 3^- state the main contribution of the corresponding expansion comes from the vector

$$||n_h = 10, \mu_h = 1, j_h^{-1} = 3^-\rangle \ , |2, \mu_p = 1, j_p = 0\rangle \ ; J = 3^-\rangle \qquad (8)$$

However the wave function $||n_h = 10, \mu_h = 1, j_h^{-1} = 3^-\rangle\ )$ which is observed at 2.75 MeV in the spectrum of ^{90}Zr, is not accounted for by our and many other models [1,2]. Such a feature possibly indicates the presence of strong admixtures of configurations outside the model space of proton holes.

The second exception has to do with the large density of the observed 2^+ states above 2 MeV. If the existence of all these states are confirmed at future experimental studies, then the good agreement between theory and experiment could be partially destroyed. In such a case the possibility of improving the results is to choose the $(d_{5/2})^2$ matrix elements of the two neutron interaction so as to reproduce these levels. The inclusion of these matrix elements as parameters would result in parametrized hamiltonian with a considerable number of adjustable parameters. The reason for not adopting an extensive

parametrization of the effective hamiltonian in the present work is because we are interesting to determine nuclear spectra with a hamiltonian that has some claim on microscopic justification.

As concerns the spectrum of ^{92}Mo the agreement between theory and experiment is quite good for both negative and positive parity states. Our model accounts for the first excited states 3^-, 5^-, 1^-, 7^-, 4^+, 6^+ and 8^+ to within 50-400 keV.

Finally, in Fig.12 and Fig.13 we show the predictions for the calculation of the energy spectra ^{97}Rh, ^{91}Y and ^{90}Y [13,17,21]. The experimental information on the first of these nuclei are still very uncertain in the spin and parity assignements. For this reason, any comparison between experiment and theory can only be considered as tentative. As Fig.12 shows the calculation accounts for all observed states within 100-400 keV. Our calculation, predicts also the presence of two $11/2^+$ states at 0.81 and 1.24 MeV, while in the experimental spectrum there appears one possible $11/2^+$ state at 1.24 MeV. On the other hand, one should notice that in the experimental spectrum there are two possible $5/2^-$ states at 0.85 and 1 MeV respectively, while our model in this energy region can account for only one such state at 1.15 MeV. Thus the second state is predicted by the calculation to be at around 2 MeV. It would be interesting therefore, if more experimental information became available for the existence or not of the above states, that the predictions of the model could be further tested.

Unlike the case of ^{97}Rh discussed above, the calculated excitation energies of ^{91}Y as well as ^{90}Y are not in satisfactory agreement with the experimental ones [17,21], specifically of those with positive parity, which appear to be between 400 and 800 keV lower than the experimental states. The failure of the calculation to explain satisfactorily the observed spectra of ^{91}Y can be attributed to the following reasons:
i) To errors in the effective two body interaction
ii) To the possible presence of strong three body effective forces which have not been considered here. Such an effective three body interaction would have stronger effects in nuclei which are found in the middle of the shell, since the three body interaction grows much faster with the number of valence particles than does the two body one.
iii) To the presence of configurations outside the model space among which are those that arise from excitations of one or more proton holes to the $g_{7/2}$, $d_{5/2}$, $d_{3/2}$, $s_{1/2}$ and $h_{11/2}$ orbitals. The inclusion of such configurations possibly will improve the calculated first excited $9/2^+$ state in ^{89}Y, which appear to have the main contribution in the construction of positive parity states in both ^{91}Y and ^{90}Y according to the weak coupling approximation we have adopted.

We conclude this section by comparing the predictions of the calculation of the

electromagnetic decay properties of the $N = 51 - 52$ nuclei with experimental data. Such a comaprison is made in Table 3. The theoretical results of Table 3 have been determined using effective proton and neutron matrix elements, calculated by perturbation theory, as it was mentioned in sec.2. Thus the results have been obtained without the use of any adjustable parameters.

As may be seen in Table 3, the results of the caculation of electromagnetic decay rates of the low lying states are, generally, in very satisfactory agreement with experiment. However there are some interesting features to be observed in the calculation of the transition probabilities. As we can see in Table 3, four out of five B(M1) probabilities in the spectrum of ^{92}Nb, are in disagreement with the experimental estimations. One should note that the experimental B(M1) values are very small quantities. This indicates that even a small change in the wavefunctions of these states could improve the agreement between theory and experiment. The same feature can be observed in the M1 transition $9/2^+ \rightarrow 7/2^+$ of ^{93}Mo. It is worth noting also that on the transistion $3^- \rightarrow 2^-$ of ^{90}Y which is a mixture of M1 and E2 there is an experimental estimate for the M1 transition but not for the corresponding E2. However the multipole mixing ratio $\delta(E2/M1)$ for this particular transition has been measured and its value is δ=-0.04 ± 0.04. The calculated value for this quantity is -0.03, which is in very good agreement with the experimental data. Similary results we have for the transition $7^+ \rightarrow 3^-$ of ^{90}Y which is a mixture of E5 and M4. The calculated value of δ which is 5.3×10^{-3} lies within the experimental estimate.

However, one should remark that to check properly the validity of a calculation, like the present one, many more experimental data on the decay properties of the $N = 51 - 52$ nuclei are required. Generally as may be observed in this table, there is a good agreement of the theory predictions with the experimental data. Such a feature certainly increses the confidence on the validity of the model employed in the calculation.

4 Conclusions

On the 17 nuclei examined in the present calculation, the worst agreement with experiment was observed for the nuclei ^{90}Y and ^{91}Y. This disagreement could be attributed possibly to the presence in the low lying states of these nuclei of configurations outside the model space of proton holes. Such a possibility is also supported by the fact that our calculation fails to account for the first excited 3^- state in ^{92}Zr, although it reproduces the rest of the spectrum in a very satisfactory manner.

One of the most serious problems in the present study on the $N = 51 - 52$

nuclei is the lack of detailed experimental information for these nuclei. Thus as was evident from the presentation of the results in sect.3, the predictions of the calculation could be compared with experimental data only in a very tentative manner. Additional experimental information would enable us to better determine values for the parameters of our calculation and thus to improve the results.

References

[1] I. Talmi and I. Unna, Nucl. Phys. **19** (1960) 225

[2] G.M. Gazzally, N.M. Hintz, M.A. Franey, J. Dubach and W.C. Haxton Phys. Rev. **C28** (1983) 294

[3] W.C. Haxton and D. Strottman unpublished

[4] X. Ji and B.H. Wildenthal Phys. Rev. **C37** (1988) 1256

[5] X. Ji and B.H. Wildenthal Phys. Rev. **C38** (1988) 2849

[6] X. Ji and B.H. Wildenthal Phys. Rev. **C40** (1988) 389

[7] J. Sinatkas, L.D. Skouras, D. Strottman and J.D Vergados Phys. G: Nucl. Part. Phys. **18** (1992) 1377

[8] J. Sinatkas, L.D. Skouras, D. Strottman and J.D Vergados Phys. G: Nucl. Part. Phys. **18** (1992) 1401

[9] J. Sinatkas, L.D. Skouras and J.D. Vergados Phys. Rev. **C37** (1988) 1229

[10] L.D. Skouras and D. Manakos Phys. G: Nucl. Part. Phys. **19** (1993) 731

[11] L.D. Skouras and C. Dedes Phys. Rev. **C15** (1977) 1873

[12] J.P. Elliot, A.D. Jackson, H.A. Mavromatis, E.A. Sanderson and B. Singh Nucl. Phys. **A121** (1968) 241

[13] B. Haesner and P. Luksch Nucl. Data Sheets **46** (1985) 718

[14] T.W. Burrows Nucl. Data Sheets **68** (1993) 720

[15] M. Coral Nucl. Data Sheets **66** (1992) 400

[16] J.K. Tuli Nucl. Data Sheets **66** (1992) 53

[17] H.-W. Muller Nucl. Data Sheets **60** (1990) 854

[18] H. Sievers Nucl. Data Sheets **54** (1988) 160

[19] L.K. Peker Nucl. Data Sheets **68** (1993) 256

[20] A. Plochocki *et al* and the ISOLDE collaboration Z. Phys. **A342** (1992) 41

[21] L.P. Ekstrom and J. Lyttkens-Linden Nucl. Data Sheets **67** (1992) 624

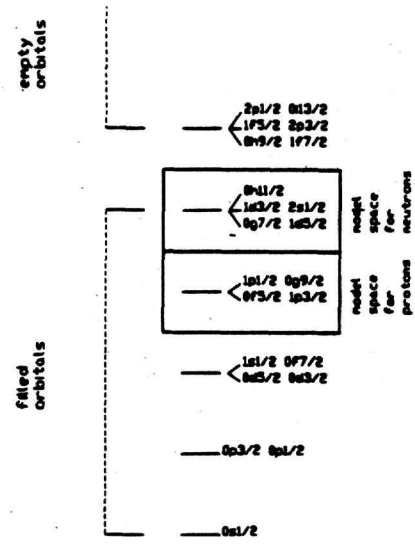

Fig. 1: Harmonic oscillator spectrum used for the determination of matrix elements elements of effective operators. The rectangular boxes enclose the orbitals of the model spaces for protons and neutrons.

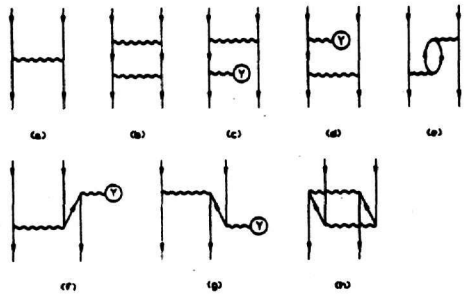

Fig. 2: Diagrams considered in the determination of the two proton hole effective interaction.

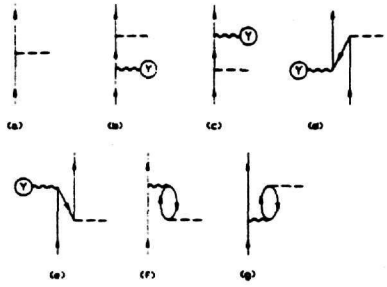

Fig. 3: Diagrams considered in the determination of the effective operators between one neutron states.

Table 1

Matrix elements $\langle j_1^{-1} j_2^{-1}; J|V|j_3^{-1} j_4^{-1}; J\rangle$ (in MeV)
for proton-holes in the model spaces $model-1$ and $model-2$

$2j_1$	$2j_2$	$2j_3$	$2j_4$	J	$model-1$	$model-2$
9	9	9	9	0	-1.4872	-1.5090
				2	-0.7134	-0.7888
				4	-0.2088	-0.2111
				6	-0.0345	0.0099
				8	0.0905	0.1430
9	9	1	1	0	0.9346	0.9313
9	9	1	3	2	-0.3546	-0.3432
9	9	3	3	0	1.2870	1.3193
				2	0.4011	0.4381
9	1	9	1	4	0.0570	0.0919
				5	-0.4269	-0.4088
9	1	9	3	4	0.1246	0.1460
				5	-0.4340	-0.4678
9	3	9	3	3	-0.8119	-0.8734
				4	-0.0158	0.0139
				5	-0.1172	-0.0776
				6	0.1193	0.1705
1	1	1	1	0	-0.1476	-0.1421
1	1	3	3	0	-1.4767	-1.4936
1	3	1	3	1	0.1850	0.2354
				2	-0.7612	-0.7338
1	3	3	3	2	0.5872	0.5988
3	3	3	3	0	-1.2370	-1.2016
				2	-0.4374	-0.3976

Table 2
matrix elements $\langle j_1 \| T^L \| j_2 \rangle$ † for neutron particles in the model spaces $moddel-3$ and $model-4$

T^L	$2j_1$	$2j_2$	Bare	$model-3$	$model-4$
M1	7	7	2.3283	1.3182	1.3182
	7	5	0.	0.2295	0.2295
	5	5	-2.7052	-1.8573	-1.8573
	5	3	-2.8920	-3.9538	-3.9538
	3	3	1.4460	1.0194	1.0194
	3	1	0.	0.1042	0.1042
	1	1	-2.2863	-1.5775	-1.5775
	11	11	-3.5150		-2.5098
E2	7	7	0.	-12.581	-16.421
	7	5	0.	3.7737	4.1339
	7	3	0.	-10.033	-11.369
	5	5	0.	-7.5161	-8.9618
	5	3	0.	-3.7466	-4.6874
	5	1	0.	-6.2060	-7.4969
	3	3	0.	-5.6497	-7.0619
	3	1	0.	5.1973	6.2825
	11	11	0.		-13.300

† EL matrix elements are expressed in units of $e(fm)^L$ while ML in units $\mu_\nu(fm)^{(L-1)}$

Table 2
Continued

T^L	$2j_1$	$2j_2$	Bare	*model*−3	*model*−4
M3	7	7	-96.533	-43.623	-47.987
	7	5	-57.035	-77.990	-88.559
	7	3	-49.394	-44.510	-49.874
	7	1	0.	-14.390	-23.055
	5	5	210.43	158.79	137.56
	5	3	114.54	140.93	153.65
	5	1	215.61	182.97	164.63
	3	3	-35.072	-33.901	-39.661
	11	11	271.26		179.40
E4	7	7	0.	281.27	368.21
	7	5	0.	-183.62	-217.98
	7	3	0.	189.01	226.14
	7	1	0.	-195.54	-221.60
	5	5	0.	158.21	188.77
	5	3	0.	222.91	271.92
	11	11	0.		299.88
E3	7	11	0.		-32.874
	5	11	0.		75.305
M4	7	11	-1619.4		-915.47
	5	11	1536.3		1709.6
	3	11	-2410.4		-2273.5
M2	7	11	45.266		23.074
E5	7	11	0.		1041.7
	5	11	0.		-1190.7
	3	11	0.		874.67
	1	11	0.		-1109.5

Table 3
Reduced Transition Probabilities B(QL) in the $N = 51 - 52$, $39 \leq Z \leq 47$ nuclei

QL	Nucl	$J_i^{\pi *}$	E_i †	$J_f^{\pi *}$	$E_f^{\dagger}$	Exper ‡	Ref.	Calc
M1	^{94}Tc	6^+	102	7^+	0		[17]	0.68
		5^+	210	6^+	102			0.65
	^{93}Mo	7^+	1363	5^+	0	$(6.8\pm0.6)\times10^{-2}$	[19]	7×10^{-2}
		9^+	1477	7^+	1363	$(27\pm13)\times10^{-5}$		0.04
		7^+	1520	5^+	0			0.10
		5^+	1695	7^+	1363	0.56 ± 0.06		0.14
		13^-	2450	11^-	2440	0.7		0.04
	^{92}Nb	3^+	285	2^+	135	$(5\pm3)\times10^{-3}$	[16]	0.78
		3^-	389	2^-	225	> 0.0004		0.03
		4^+	480	5^+	357	$(4.4\pm0.9)\times10^{-3}$		1.00
		6^+	501	7^+	0	$(5\pm8)\times10^{-4}$		0.43
		4^+	480	3^+	285	$(3.4\pm0.6)\times10^{-3}$		1.65
	^{91}Zr	7^+	1882	5^+	0	0.022^{+10}_{-19}	[18]	0.13
		5^+	1466	5^+	0	$(37\pm18)\times10^{-3}$		44×10^{-3}
		3^+	2042	5^+	0	0.23 ± 0.02		0.80
		7^+	2200	5^+	0	$(48\pm26)\times10^{-4}$		34×10^{-4}
		15^-	2287	13^-	2259	$(34\pm13)\times10^{-3}$	[22]	42×10^{-3}

*For odd mass nuclei the value quoted corresponds to 2J
†In keV
‡In Weisskopf units

Table 3
Continued

QL	Nucl	$J_i^{\pi *}$	E_i †	$J_f^{\pi *}$	$E_f^{\dagger}$	Exper ‡	Ref.	Calc
	^{90}Y	3^-	205	2^-	0	$(102\pm3)\times10^{-4}$		136×10^{-4}
E2	^{94}Tc	6^+	102	7^+	0		[17]	4.45
		5^+	210	6^+	102			0.15
	^{95}Ru	17^+	2284	13^+	2029	6.4±0.6	[15]	0.95
		21^+	2539	17^+	2284	1.94±0.05		1.12
	^{93}Mo	7^+	1363	5^+	0	8.7±2.4	[19]	4.62
		9^+	1477	5^+	0	12±4		8.02
		9^+	1477	7^+	1363			0.97
		7^+	1520	5^+	0			6.42
		13^+	2161	9^+	1477	3.6±0.3		4.88
		17^+	2429	13^+	2161	4.64±0.24		2.20
E2	^{92}Nb	3^+	285	2^+	135	1.2±0.9	[16]	3.84
		5^+	357	7^+	0	2.03±0.05		1.42
		3^-	389	2^-	225	> 0.16		0.96
		4^+	480	5^+	357	0.6±0.7		0.49
		11^-	2203	9^-	2080	3.92±0.11		2.60
	^{91}Zr	1^+	1204	5^+	0	54±19	[18]	5.48
		7^+	1882	5^+	0	6^{+6}_{-3}		11.5
		3^+	2042	5^+	0	60±5		1.75
		9^+	2131	5^+	0	4.4±0.7		5.46
		7^+	2200	5^+	0	0.9±0.5		0.50
	^{90}Y	3^-	205	2^-	0		[22]	0.21

Table 3
Continued

QL	Nucl	$J_i^{\pi *}$	E_i †	$J_f^{\pi *}$	$E_f^{\dagger}$	Exper ‡	Ref.	Calc
M3	^{96}Rh	3^+	52	6^+	0	1.49±0.14	[20]	1.07
E3	^{91}Zr	11^-	2170	5^+	0		[18]	4.79
		21^+	3167	15^-	2288	$(5.4\pm0.6)\times10^{-2}$		0.44
M4	^{90}Y	7^+	682	3^-	202	1.58±0.05	[22]	4.01
E4	^{93}Mo	21^+	2424	13^+	2161	1.45±0.01	[19]	0.03
E5	^{90}Y	7^+	682	3^-	202		[22]	1.68
		7^+	682	2^-	0	1.75±0.16		2.47
M1	^{95}Tc	3^-	646	1^-	38	$0.073\leq B(M1)\leq0.39$	[14]	0.23
		3^+	927	5^+	626	≤ 0.60		0.38
		11^+	957	9^+	0	$(3.5^{+0.9}_{-1.5})\times10^{-3}$		2.8×10^{-3}
		7^+	1178	5^+	626	$0.09^{+0.03}_{-0.05}$		0.11
	^{96}Ru	2^+	1931	2^+	832	$(15\pm6)\times10^{-4}$	[19]	270×10^{-4}
	^{94}Mo	2^+	1864	2^+	871	$(32\pm18)\times10^{-3}$	[16]	58×10^{-3}
	^{93}Nb	3^-	687	1^-	30	$0.3^{+0.1}_{-0.2}$	[18]	0.16
		7^+	743	9^+	0	$0.09^{+0.02}_{-0.01}$		0.02
		11^+	979	9^+	0	$0.081^{+0.010}_{-0.009}$		0.04
		9^+	1082	7^+	743	<0.16		0.05
		9^+	1082	9^+	0	$<1.1\times10^{-3}$		1.8×10^{-3}
E2	^{95}Tc	3^-	646	1^-	38		[14]	9.82
		13^+	882	9^+	0	34^{+15}_{-32}		9.53
		3^+	927	5^+	626	<360		3.66
		11^+	957	9^+	0	17^{+4}_{-7}		5.92
		7^+	1178	5^+	626	14 ± 14		2.32
		11^+	1307	7^+	336	27 ± 8		5.55

Table 3
Continued

QL	Nucl	$J_i^{\pi *}$	E_i †	$J_f^{\pi *}$	$E_f^{\dagger}$	Exper ‡	Ref.	Calc
	^{96}Ru	2^+	832	0^+	0	18±6	[19]	7.98
		4^+	1518	2^+	832	21±3		8.51
		2^+	1931	2^+	832	33±6		10.9
		0^+	2148	2^+	832	12±8		1.29
		6^+	2149	4^+	1518			6.31
	^{94}Mo	2^+	871	0^+	0	15.42±22	[16]	10.2
		4^+	1573	2^+	871	26±4		11.5
		2^+	1864	2^+	871	130±50		16.8
		2^+	2067	0^+	0	1.9±0.5		1.11
		8^+	2955	6^+	2872	3.8±1.0		4.71
E2	^{93}Nb	3^-	687	1^-	30	11±7	[18]	9.11
		7^+	743	9^+	0	8.8±0.3		15.6
		13^+	949	9^+	0	6.70±0.23		8.40
		11^+	979	9^+	0	13±7		10.0
		9^+	1082	7^+	743	<69		11.6
		9^+	1082	9^+	0			0.24
	^{92}Zr	2^+	934	0^+	0	6.4±0.6	[15]	11.8
		0^+	1382	2^+	934	14.3±0.5		10.7
		4^+	1495	2^+	934	4.04±0.12		10.8
M3	^{95}Tc	13^+	882	9^+	0		[14]	0.01
M4	^{95}Tc	1^-	38	9^+	0	15.6±1.6		93.3
	^{93}Nb	1^-	30	9^+	0	11.1±0.7	[18]	48.3
	^{97}Rh	1^-	258	9^+	0	22±3	[13]	94.2

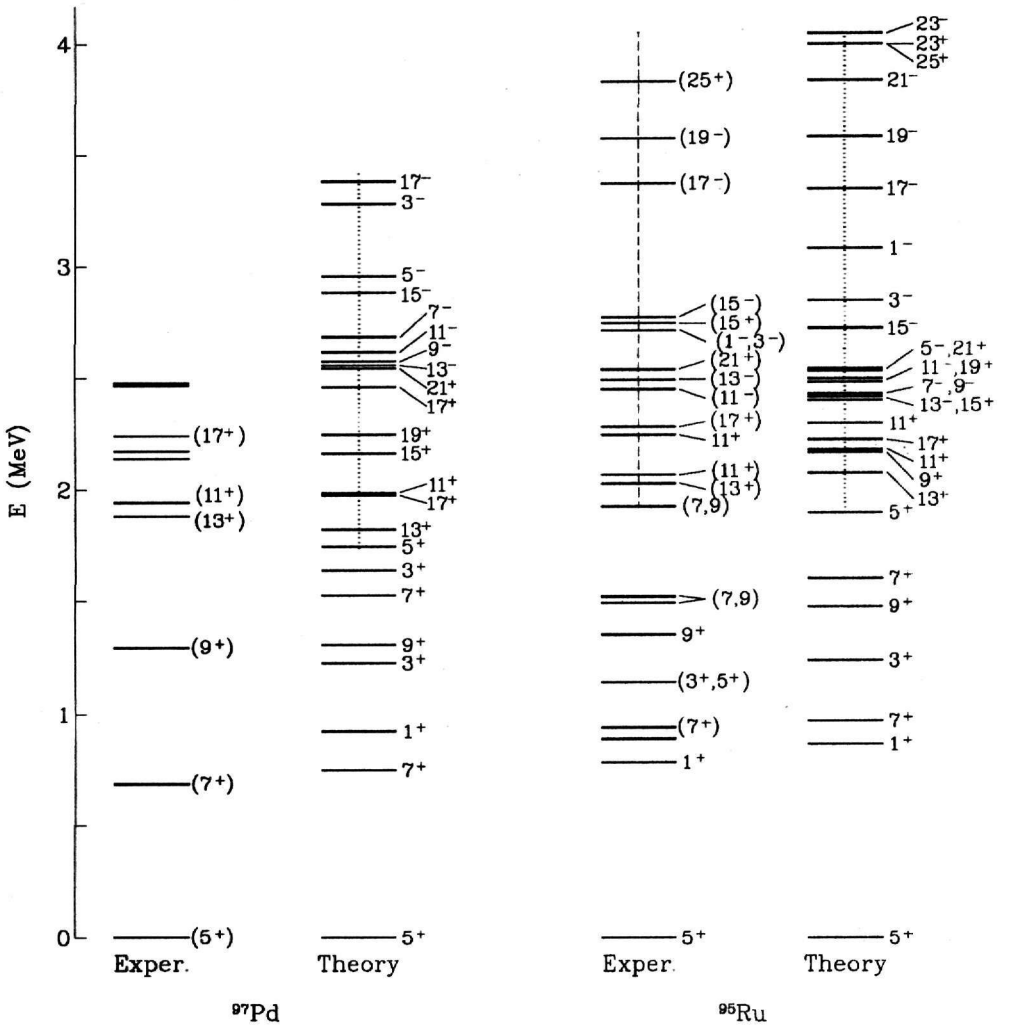

Fig. 4: Theoretical and experimental spectra of ^{97}Pd and ^{95}Ru [13,14]. The dashed line in the experimental spectra indicates that there are states of unidentified spin and parity. The dot line in the theoretical spectra indicates the presence of other states not shown in the figure. For odd mass nuclei each lavel is labelled by 2J.

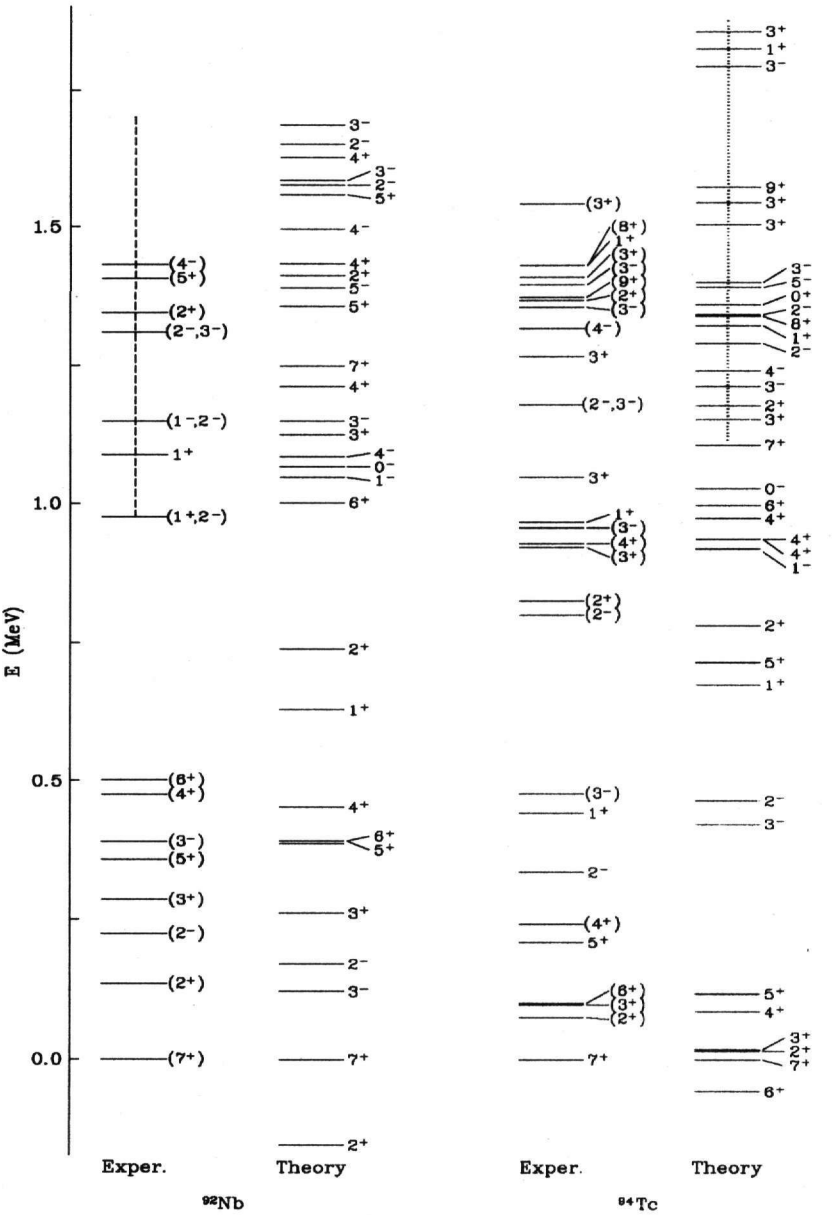

Fig. 5: Theoretical and experimental spectra of ^{92}Nb and ^{94}Tc [15,16].

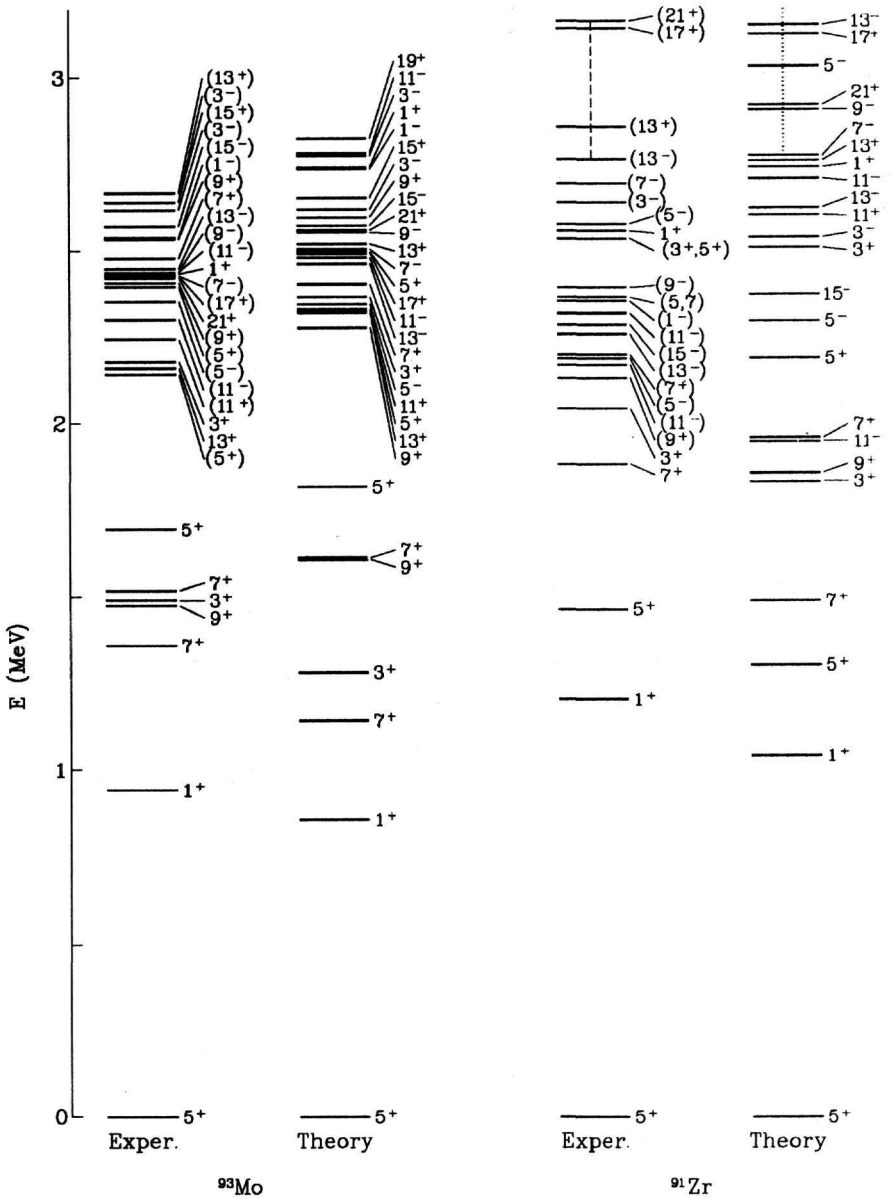

Fig. 6: Theoretical and experimental spectra of ^{91}Zr and ^{93}Mo [17,18].

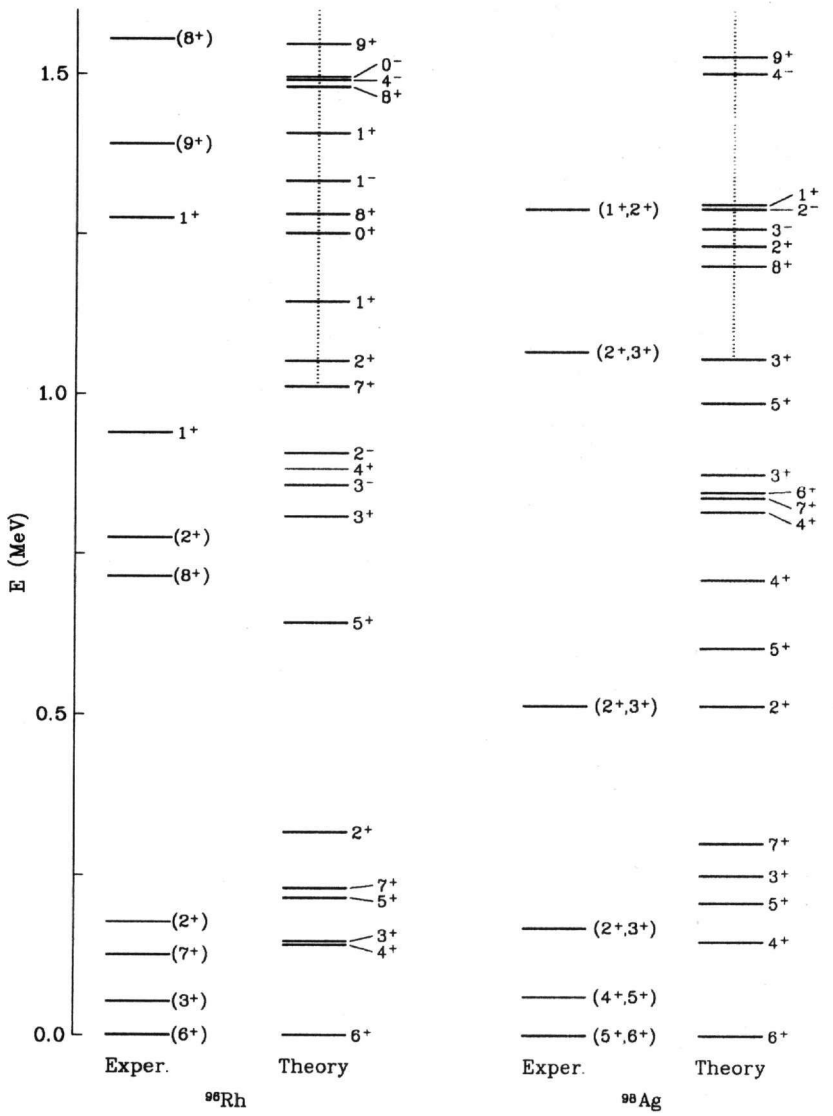

Fig. 7: Theoretical and experimental spectra of ^{96}Rh and ^{98}Ag [19,20].

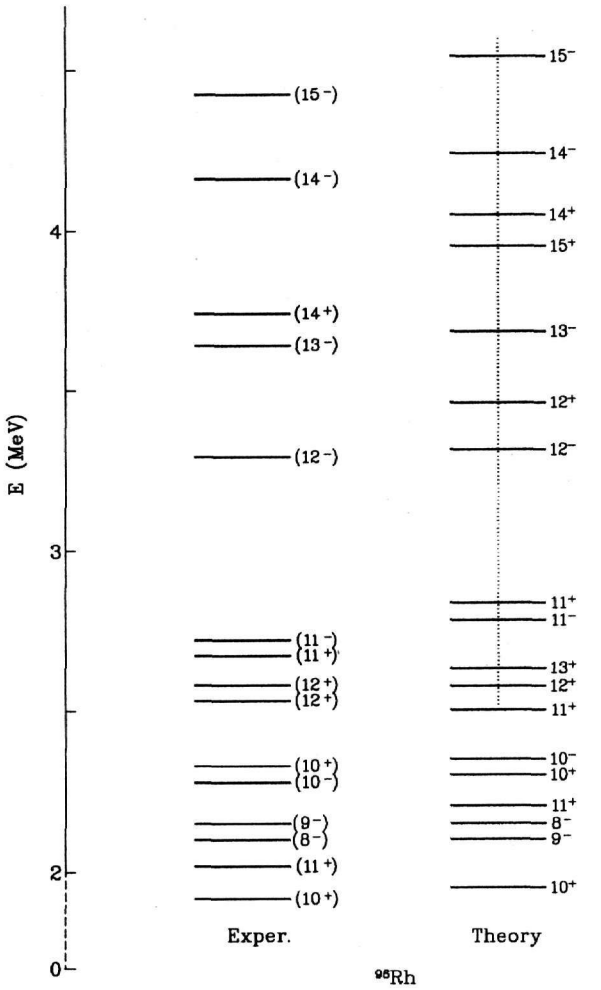

Fig. 8: Theoretical and experimental spectrum of ^{96}Rh above 2 MeV.

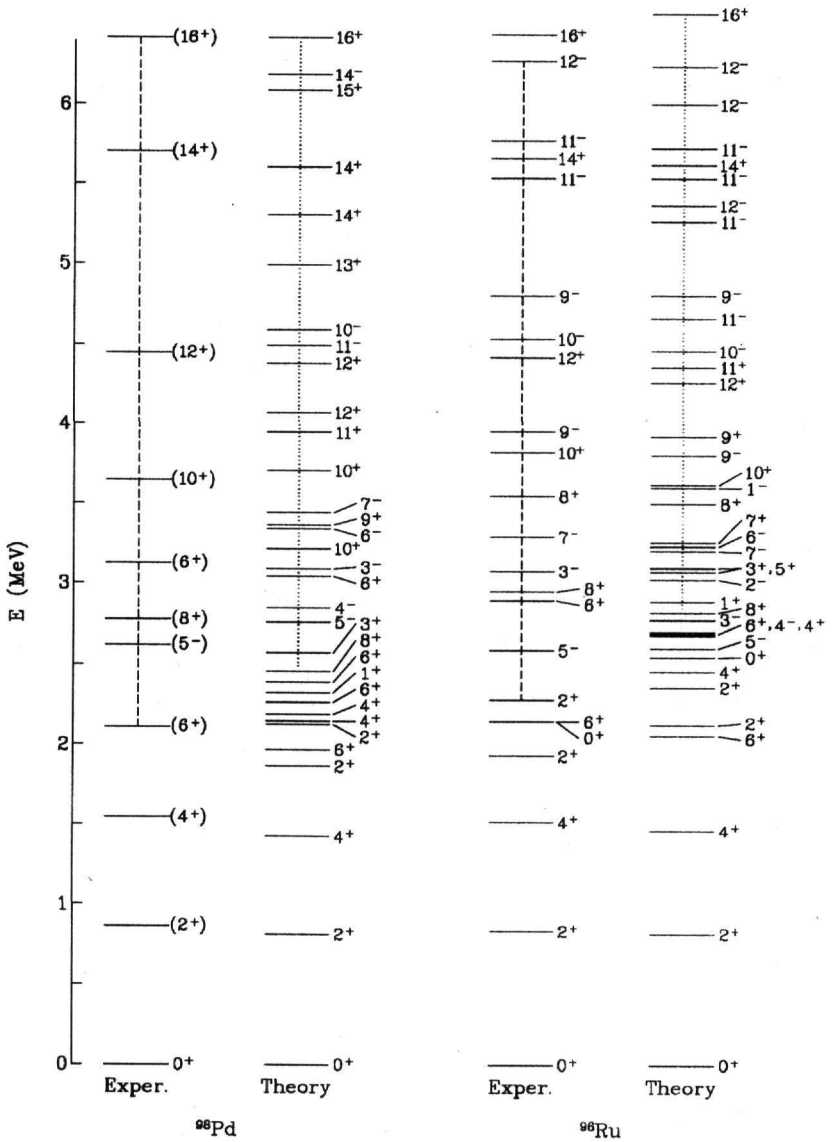

Fig. 9: Theoretical and experimental spectra of ^{98}Pd and ^{96}Ru [20,19].

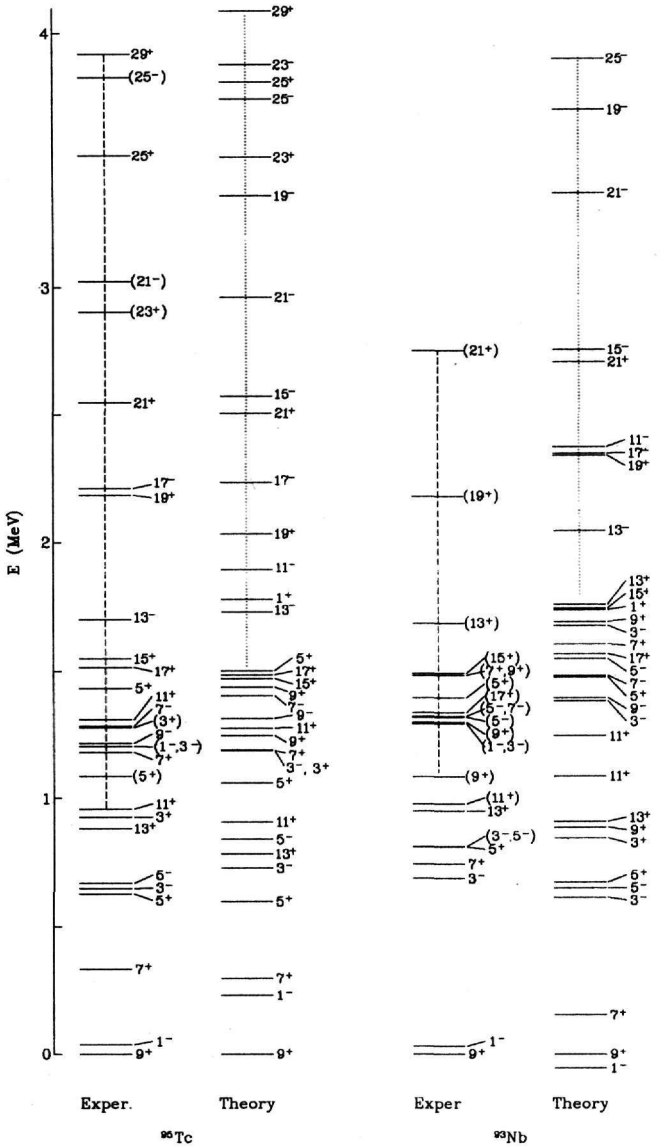

Fig. 10: Theoretical and experimental spectra of ^{95}Tc and ^{93}Nb [14,18].

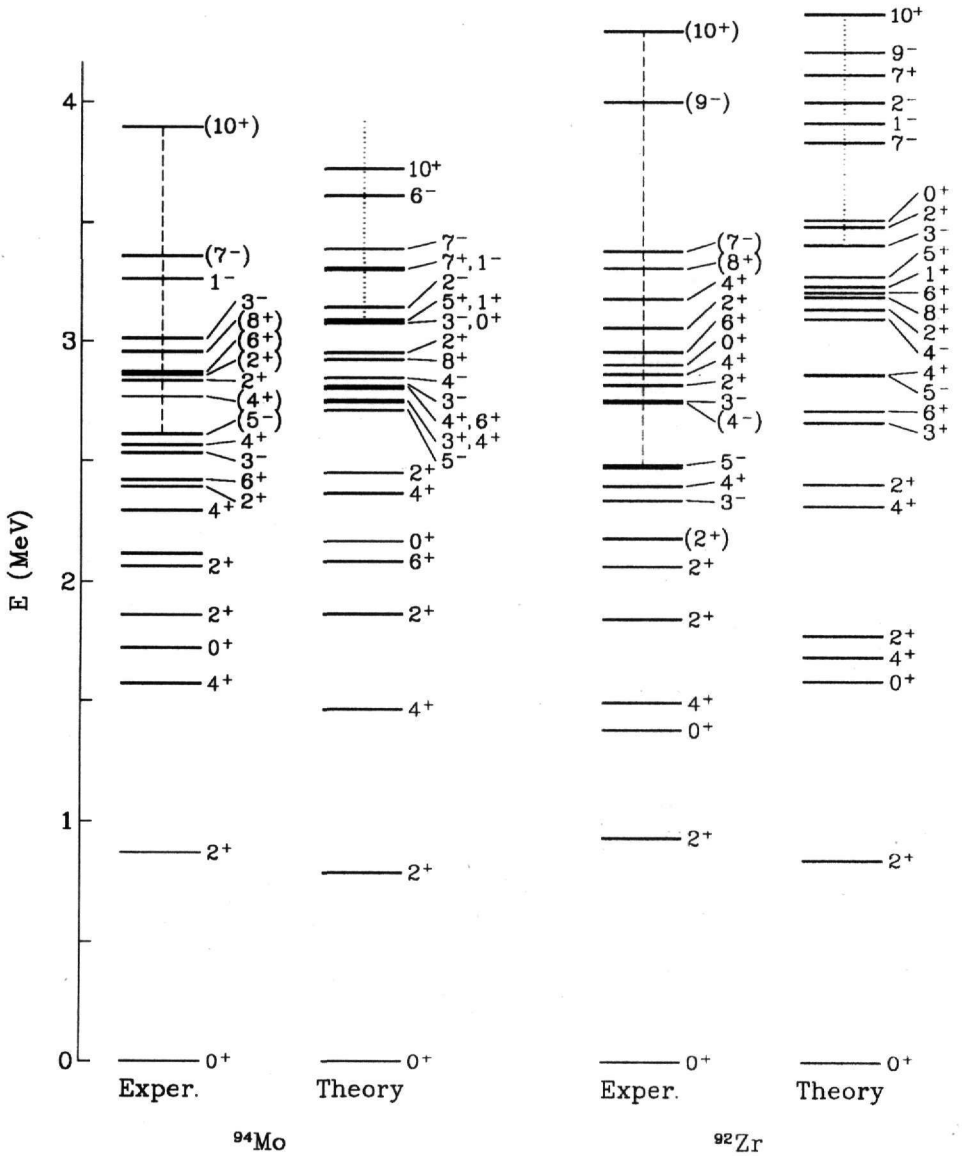

Fig. 11: Theoretical and experimental spectra of ^{92}Zr and ^{94}Mo [15,16].

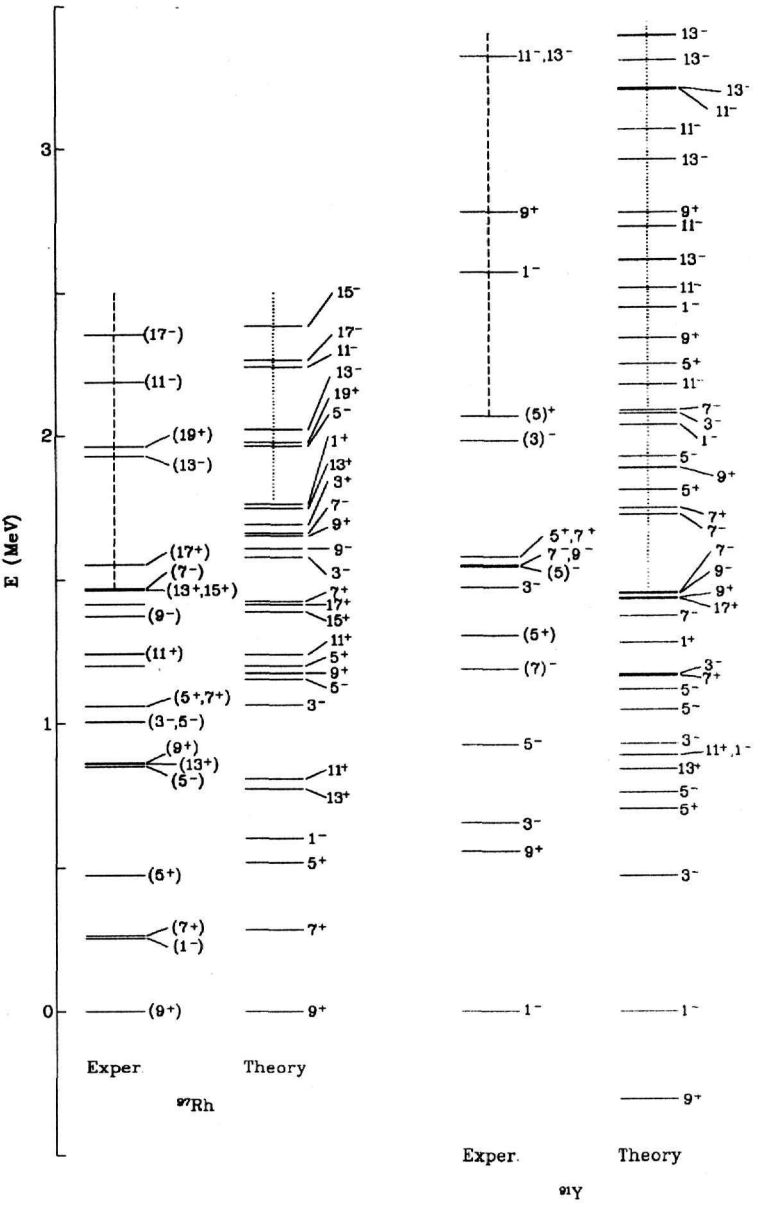

Fig. 12: Theoretical and experimental spectra of ^{97}Rh and ^{91}Y [13,17].

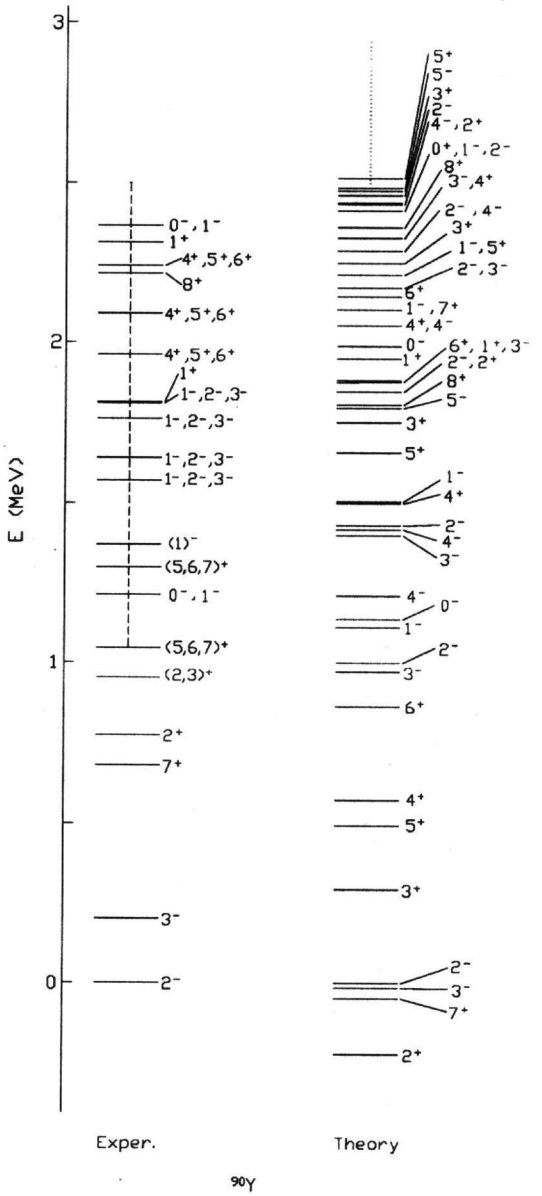

Fig. 13: Theoretical and experimental spectrum of ^{90}Y [21].